Controller design of a new active front steering system

DELING CHEN, CHENGLING YIN, JIANWU ZHANG
Institute of Automotive Engineering, School of Mechanical Engineering
Shanghai Jiao Tong University
No.800 DongChuan Road, Minhang District, Shanghai City
P.R.China
E-mail address: chendeling_sh@hotmail.com

Abstract: - An AFS (active front steering) on the basic of a C-EPS (column electric power steering) system was developed. Based on the mathematical model of essential components, the AFS controller was designed covering two units: an EPS actuator unit was used to reduce the steering torque requirement to the driver; an AFS actuator unit was used to compensate the steering angle for steering characteristics and vehicle stability. In contrast to the conventional stability control, both the sideslip angle and the yaw rate were fed back to this AFS controller and the stability performance has been optimized with LQR (linear quadratic regulator). In addition, tire stiffness uncertainties have been taken account in the LQR controller to provide the control robustness. Finally, HILS (Hardware-in-the-Loop Simulation) tests were conducted to demonstrate the performance of the designed AFS controller. Experiment indicates that the proposed AFS system can improve vehicle stability and compensate the steering reaction torque effectively.

Key-Words: - Active front steering (AFS), Electric power steering (EPS), Linear quadratic regulator (LQR), Sideslip angle, Yaw rate, Vehicle stability

1 Introduction

Active Front Steering (AFS) systems have been introduced to improve handling stability under adverse road conditions. In contrast to a conventional steering system, the mechanical linkage between the steering wheel and the front wheels of an AFS system is complemented by an extra angle augment motor. Therefore, a small auxiliary front wheel angle, in addition to the steering angle imposed by the driver, can be applied to stabilize the vehicle besides improving vehicle steering responses and avoiding critical handling situations. Yet, the driver can still receive information about road friction and vehicle stability directly through the mechanical linkage without the additional control as in the steer-by-wire (SBW) systems.

Additionally to the enhanced dynamic behavior of the steering system and vehicle stabilization, the AFS system should also provide an improved steering comfort by reducing steering effort [1]. Therefore, the torque assistance is required to limit manual forces to a reasonable level. The existing AFS system used the commercially available hydraulic power assisted steering system with which the oil volumetric flow should be adapted to the output requirements. Then an additional flow control valve was usually used resulting in a complex control concept [2].

This new developed AFS is based on a column electric power steering system (C-EPS). Therefore, the construction can vary the steering ratio by superimposing steering angle and alleviate the steering torque requirement to the driver by the EPS actuator. The actuator can provide directional control to the vehicle drive and reduce the engine load in contrast to the hydraulic power assisted AFS system. Furthermore, complex hydraulic system and hydraulic delay can be eliminated. Therefore, two motors are included in the AFS system. One provides augment of the steering wheel angle, while another in the EPS system provides the torque assistance.

The goal of this paper is to develop an AFS controller, which not only helps ensure the vehicle's response operability matching the driver's sense, but also helps prevent the vehicle from falling into an unstable state. Most stability researches used only the yaw rate to improve the vehicle handling stability due to the difficulties associated with the sideslip angle measurement [3, 4]. Theoretically, the lateral motion of the vehicle is described by yaw rate and sideslip angle. In addition, the sideslip angle control can compensate the path deviation occurring from the yaw rate control. Therefore, the sideslip angle will be estimated and used to this AFS system control together with the yaw rate.

To achieve better vehicle stability, the state parameters of driving vehicle should be fed back. The linear quadratic regulators (LQR) can be used to find a suitable state feedback and optimize the control. LQR has been widely used due to its simple math disposal process and achieved optimal control of the closed loop. However, LQR design provides the optimal gain, which is a function of the system matrices. Unfortunately, some parameter uncertainties exist in the vehicle system, and result in model inaccuracy. Therefore, although some inherent robustness properties exist, the classical LQR controller is not robust enough to system uncertainties and cannot guarantee the stability of the actual system [5].

Therefore, the classical LQR control should be modified to overcome the limitations. The uncertainties appearing in the problem under consideration include unmodeled dynamics, parameter perturbations and external disturbance [6]. As has been introduced in the literature of L. Gianone, an active 4WS system was designed with physical uncertainties. However, the system they designed was only for the rear tyre stiffness uncertainty that simply affected the state matrix $\boldsymbol{A}$. It is inadequate to the front wheel steering vehicle, especially the AFS vehicle. Therefore, LQR controller designed here proposed a matrix $\boldsymbol{R}$ with parameter uncertainties and applied it to the AFS control system.

The paper is organized as follows. Firstly, the structure and modelling of the developed AFS system is described. Then the control system including the EPS actuator and AFS actuator is designed based on the models in section 3. In section 4, details of the AFS control has been presented. To evaluate the designed controller, a hardware-in-the-loop simulation (HILS) system is described in section 5 and HILS tests are finally conducted in section 6. Conclusions of this paper are summarized in section 7.

2 Structure and modeling of an AFS system

The AFS system we developed is based on a column electric power steering system (C-EPS). Therefore, two motors are included, as illustrated in Fig.1: one in the original EPS system provides the power assistance to limit manual forces to a reasonable level, whereas the permanent-magnet synchronous motor (PMSM) provides augment of the steering wheel angle. Therefore, the system can be divided into two parts: EPS actuator and AFS actuator.

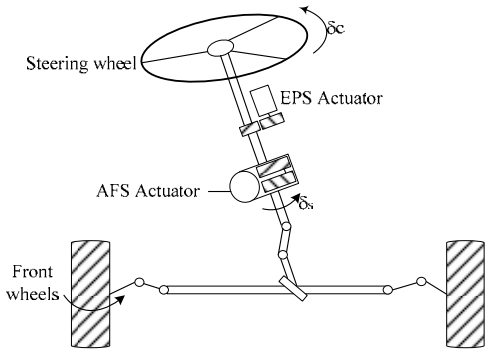

Fig.1. Structure of the active steering system

2.1 EPS actuator

A DC motor is used as EPS actuator to provide the assistant torque for its maximum torque per given current and controllable torque. The electric equation for a DC motor is [7]:

$$R_{dc} i_{dc} + K_E \dot{\delta}_{dc} = u_{dc} \quad (1)$$

where R_{dc} is the armature resistance, K_E the armature back emf constant, i_{dc} the DC motor current, u_{dc} the motor terminal voltage, δ_{dc} the angular position of the motor shaft.

The assistant torque of the EPS actuator is applied to the steering system by a worm and worm wheel. The dynamics of the DC motor then can be given by:

$$J_{dc}\ddot{\delta}_{dc} + B_{dc}\dot{\delta}_{dc} + K_{dc}(\delta_{dc} - G_d\delta_c) = K_T i_{dc} \quad (2)$$

where J_{dc}, B_{dc}, K_{dc} are the inertia moment, damping coefficient, torsional stiffness of the DC column, respectively; K_T is the motor torque constant, δ_c the steering wheel angle, G_d the gear ratio of the DC motor to the steering column.

2.2 AFS actuator

A PMSM is used as AFS actuator to provide the assistant angle for its precise motor positioning control as well as fast ratio change to the target one. The PMSM model can be described with simplification and Park's transformation [8]:

$$L'\dot{i}_q(t) = -N\sqrt{\frac{3}{2}}\lambda_m\dot{\delta}_m(t) - Ri_q(t) + u_q(t) \quad (3)$$

where L' is the stator inductance, N the number of poles, i_q the current of q-component, u_q the stator voltage of q-component, δ_m the PMSM steering angle, λ_m the magnitude of the flux created by the permanent magnets, R the armature resistance.

The torque produced by the PMSM can be expressed with simplification as:

$$T_{m2}(t) = N\sqrt{\frac{3}{2}}\lambda_m i_q(t) \tag{4}$$

The augmentation steering angle of the AFS actuator is applied to the steering column through a planetary gear mechanism, as shown in Fig.2. The planetary gear mechanism makes it easy to realize the variable steering ratio (VSR) and produce superimposed steering angle.

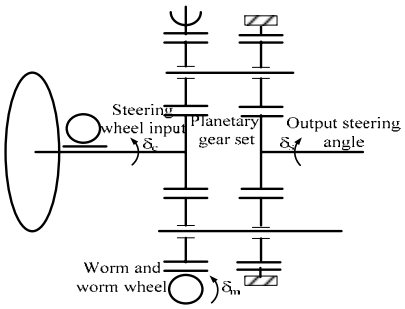

Fig.2. Schematic of the planetary gear mechanism

Thus, the superimposed angle is:

$$\delta_s = \frac{1}{i_s}\delta_c + \frac{1}{i_m}\frac{\delta_m}{G_h} \tag{5}$$

where i_s is the gear ratio of the steering column to sun wheel of the planetary gear set, i_m the gear ratio of PMSM to the ring of the planetary gear set, G_h the gear ratio of worm-to-worm wheel, δ_s the superimposed angle of the steering column.

The PMSM dynamics can be described as [9]:

$$J_m\ddot{\delta}_m + B_m\dot{\delta}_m + (\frac{K_c i_s^{\,2}}{(G_h i_m)^2} + K_m)\delta_m + (\frac{K_c i_s}{G_h i_m} + \frac{K_m G_h i_m}{i_s})\delta_c + (-\frac{K_c i_s^2}{G_h i_m r_p} - \frac{K_m G_h i_m}{r_p})p = T_{m2} \tag{6}$$

where J_m, B_m, K_m are the inertia moment, damping coefficient, torsional stiffness of PMSM column, respectively; K_c the torsional stiffness of steering column, p the displacement of the rack and tie rod, r_p the radius of the pinion.

2.3 Steering mechanics

Steering mechanics are also included in the system, such as steering column, rack and tie rod. The dynamic equations for the steering system besides the EPS and AFS actuator can be expressed as [9]:

$$J_c\ddot{\delta}_c + B_c\dot{\delta}_c + (K_c + G_d^2 K_{dc} + (\frac{G_h i_m}{i_s})^2 K_m)\delta_c - K_{dc}G_d\delta_{dc} + (\frac{K_c i_s}{G_h i_m} + \frac{K_m G_h i_m}{i_s})\delta_m + (-\frac{K_c i_s}{r_p} - \frac{K_m G_h^{\,2} i_m^{\,2}}{i_s r_p})p = T_d \tag{7}$$

$$m_r\ddot{p} + B_r\dot{p} + (\frac{K_c i_s^2}{r_p^{\,2}} + K_m(\frac{G_h i_m}{r_p})^2 + K_t)p + (-\frac{K_c i_s}{r_p} - \frac{K_m G_h^{\,2} i_m^{\,2}}{i_s r_p})\delta_c + (-\frac{K_c i_s^2}{G_h i_m r_p} - \frac{G_h i_m K_m}{r_p})\delta_m - K_t l_k\delta_f = 0 \tag{8}$$

$$J_w\ddot{\delta}_f + B_w\dot{\delta}_f + (K_t l_k^{\,2} + K_w)\delta_f - K_t l_k p = -M_z \tag{9}$$

where J_c, J_w are the inertia moment of the steering column, the front wheels, respectively; K_t, K_w the torsional stiffness of the steering rack and tie rod, the front wheels, respectively; B_c, B_r, B_w the damping coefficient of steering column, rack and tie rod, front wheels; δ_f the steering angle of the front wheels, m_r the mass of the rack and tie rod, l_k the length of the steering knuckle arm, T_d the torque provided by the driver, M_z the resistance moment of the front wheels.

Equation (7) describes the dynamic motion of the steering column; Equation (8) represents the dynamics of the rack and the tie rod. Equation (9) describes the dynamics of the front wheels. In Equation (9), the resistance moment of the front wheels are depend on the longitudinal velocity. When the vehicle is driven, with small sideslip angle assumption of a linear vehicle model, the resistance moment of the front wheels can be simplified as:

$$M_z = K_{af}d(\beta + \frac{a}{v_x}\gamma - \delta_f) \tag{10}$$

where K_{af} is the cornering coefficient of the front wheels, d the pneumatic trail of the front wheels, γ the yaw rate of vehicle, β the sideslip angle of vehicle, v_x the longitudinal velocity, a the distance from gravity center to front axle.

When a vehicle moves slowly on dry asphalt and changes direction, a large amount of steering torque is required due to the road load on the tyres. The tyres roll and change their directions simultaneously [10]. The maximum resistance moment determining the directional angle of front wheel can be expressed as [11]:

$$M_z = \frac{\mu}{3}\sqrt{\frac{G_1^{\,3}}{P}} \tag{11}$$

where μ is the friction coefficient between the tyre and the road, G_1 the load of the front wheels, P the pressure of the tyres.

Express the AFS actuator model in state-space form:

$$\dot{\boldsymbol{x}} = \boldsymbol{A}\boldsymbol{x} + \boldsymbol{B}\boldsymbol{u} \tag{12}$$

where, system input $\boldsymbol{u}=\begin{bmatrix}\delta_c & u_q & M_z\end{bmatrix}^{\mathrm{T}}$, the state assignment $\boldsymbol{x}=[\delta_m \quad \dot{\delta}_m \quad p \quad \dot{p} \quad \delta_f \quad \dot{\delta}_f \quad i_q]^{\mathrm{T}}$, and the control matrices are:

$$\boldsymbol{A}=\begin{bmatrix} 0 & 1 & 0 & 0 & 0 & 0 & 0 \\ a_{21} & -\frac{B_m}{J_m} & a_{23} & 0 & 0 & 0 & \sqrt{\frac{3}{2}}\frac{N\lambda_m}{J_m} \\ 0 & 0 & 0 & 1 & 0 & 0 & 0 \\ a_{41} & 0 & a_{43} & -\frac{B_r}{m_r} & \frac{K_t l_k}{m_r} & 0 & 0 \\ 0 & 0 & 0 & 0 & 0 & 1 & 0 \\ 0 & 0 & \frac{K_t l_k}{J_w} & 0 & -\frac{K_t l_k^2+K_w}{J_w} & -\frac{B_w}{J_w} & 0 \\ 0 & -\sqrt{\frac{3}{2}}\frac{N\lambda_m}{L'} & 0 & 0 & 0 & 0 & -\frac{R}{L'} \end{bmatrix}$$

$$\boldsymbol{B}=\begin{bmatrix} 0 & 0 & 0 \\ -(\frac{K_c i_s}{G_h i_m}+\frac{K_m G_h i_m}{i_s})/J_m & 0 & 0 \\ 0 & 0 & 0 \\ (\frac{K_c i_s}{r_p}+\frac{K_m G_h^2 i_m^2}{i_s r_p})/m_r & 0 & 0 \\ 0 & 0 & 0 \\ 0 & 0 & -\frac{1}{J_w} \\ 0 & \frac{1}{L'} & 0 \end{bmatrix}$$

where $a_{21}=-(\frac{K_c i_s^2}{(G_h i_m)^2}+K_m)/J_m$,

$$a_{23}=(\frac{K_c i_s^2}{G_h i_m r_p}+\frac{K_m G_h i_m}{r_p})/J_m,$$

$$a_{41}=(\frac{K_c i_s^2}{G_h i_m r_p}+\frac{G_h i_m K_m}{r_p})/m_r,$$

$$a_{43}=-(\frac{K_c i_s^2}{r_p^2}+K_m(\frac{G_h i_m}{r_p})^2+K_t)/m_r.$$

3 Control system configurations

EPS control unit and AFS control unit are included in the AFS system, as shown in Fig.3.

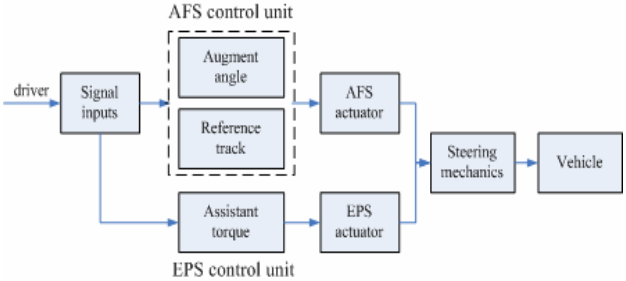

Fig.3. Block diagram of the steering system control

The EPS control unit can realize the reduction of steering torque exerted by a driver; while AFS control unit provides the steering angle augment for vehicle safety and stability. Therefore, the augment angle control and reference track control are covered in the AFS control unit.

3.1 EPS control unit

The main functions of the EPS actuator are reduction of steering torque and improvement of return-to-center performance. These two functions are not required to activate at the same time. A proper amount of assist torque should be provided to reduce the driver's steering torque during cornering, and to return the steering wheel to the original position smoothly without overshoot and subsequent oscillation of the vehicle right after reentering a straight-line road [7].

The EPS control can optimize steering effort characteristic for driver by varying a quantity of assistant torque depending on various vehicle-traveling situations, as shown in Fig.4. The target current of the motor i_r is determined based on the driving conditions to reduce the steering torque requirement. The actual current i_a is generated through the dynamics of the DC motor and the steering column, and measured by the current detecting unit. Then the controller calculates the control signal to minimize the error $e(t)$ between i_r and i_a.

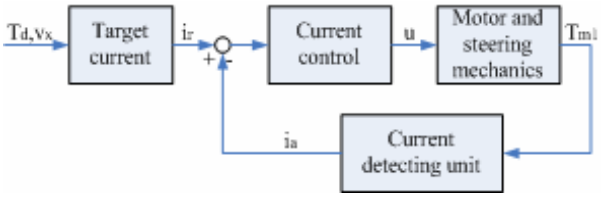

Fig.4. Control of the EPS unit

To minimize the current error, a PI control scheme is employed in the current control as:

$$u=K_p e(t)+K_i\int_0^t e(\tau)d\tau \qquad (13)$$

where K_p, K_i are the proportional gain and integral gain, respectively. Then the assistant torque is determined and delivered to the steering shaft.

3.2 AFS control unit

In order to control the AFS unit considering the VSR (variable steering ratio) and vehicle stability, a main-loop control and an inner-loop control are included in the controller, as shown in Fig.5.

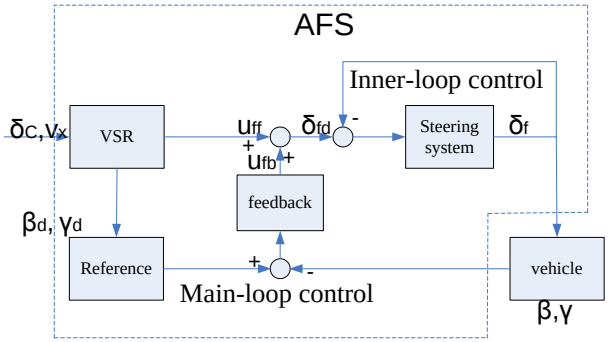

Fig.5. Control of the AFS unit

In the inner-loop control, a PI controller is design to track the target angle of the front wheel δ_{fd} with a potentiometer measuring the displacement of the steering knuckle arm. In addition, the target angle of the front wheel is determined in the main-loop control by both the feedforward and feedback control. The feedforward control determines the front wheel angle according the desired VSR and the steering wheel angle. The stability parameters are utilized in the feedback. Then the target angle can be determined in the main-loop control by the feedforward and feedback control.

4 Details of AFS main-loop control

In the main-loop control, different compensation will be applied to the front wheels to achieve desired state variables according to vehicle system dynamics. Therefore, a reference model is then established firstly.

4.1 Reference model

According to the previous researches, a simplified two-degrees-of-freedom (2DOF) vehicle model is generally derived to describe the vehicle lateral dynamics, as shown in Fig. 6 [12, 13]. Taking the sideslip angle β and the yaw rate γ as the states of the system, the 2DOF model can be described as:

$$\begin{bmatrix}\dot{\beta}\\ \dot{\gamma}\end{bmatrix}=\begin{bmatrix}-\frac{2(K_{af}+K_{ar})}{mv_x} & -\frac{2(aK_{af}-bK_{ar})}{mv_x^2}-1\\ -\frac{2(aK_{af}-bK_{ar})}{I_z} & -\frac{2(a^2K_{af}+b^2K_{ar})}{I_zv_x}\end{bmatrix}\begin{bmatrix}\beta\\ \gamma\end{bmatrix}+\begin{bmatrix}\frac{2K_{af}}{mv_x}\\ \frac{2aK_{af}}{I_z}\end{bmatrix}\delta_f \tag{14}$$

where δ_f is the steering angle controlled by the driver steering command and the variable steering ratio r, $\delta_f=\delta_c/r$; m the vehicle mass, I_z the vehicle moment of inertia; a, b are the distance from the gravity center to the front and rear axle, respectively; K_{af}, K_{ar} the cornering coefficient of the front and rear wheels, respectively.

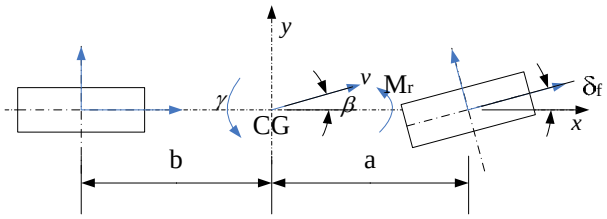

Fig.6. 2DOF vehicle model

This model represents the vehicle dynamic behavior in the linear range. Suppose the vehicle turns a constant radius circle of neutral steer, the target responses can be obtained:

$$\gamma_d=\frac{v_x/(a+b)}{(1+m((a/(2K_{ar})-b/(2K_{af}))v_x^2/(a+b)^2)}\delta_f \tag{14}$$

$$\beta_d=\left(\frac{1+(mav_x^2)/(2(a+b)\,bK_{ar})}{(1+m((a/(2K_{ar})-b/(2K_{af}))v_x^2/(a+b)^2)}\right)\frac{b}{a+b}\delta_f \tag{15}$$

Then the feedback control can regulate the compensating angle with reference values:

$$u_{fb}=K_\gamma(\gamma-\gamma_d)+K_\beta(\beta-\beta_d) \tag{16}$$

where u_{fb} is the feedback compensation voltage of the PMSM; K_γ, K_β are the feedback coefficient of γ and β, respectively.

To implement the feedback control scheme, accurate information on both sideslip angle and yaw rate are required. The sideslip angle can control the vehicle path deviation occurring from the conventional yaw rate control. The yaw rate can be measured with a gyroscope, while sideslip measurement requires expensive sensors. Therefore, estimation can serve as an option.

The sideslip angle estimation using lateral acceleration signal, which has been tested by Yoshifumi Aoki, was applied. According to the 2DOF model, the vehicle lateral acceleration a_y can be expressed as:

$$\begin{aligned}a_y&=v_x(\dot{\beta}+\gamma)\\&=v_x\left(\frac{2(K_{af}+K_{ar})}{mv_x}\beta+\frac{2(aK_{af}-bK_{ar})}{mv_x^2}\gamma-\frac{2K_{af}}{mv_x}\delta_f\right)\end{aligned} \tag{17}$$

Then, with the measurable signals a_y and γ, the estimated sideslip angle $\hat{\beta}$ is obtained:

$$\begin{aligned}\dot{\hat{\beta}}=&\frac{2(K_{af}+K_{ar})}{mv_x}\hat{\beta}+\left(\frac{2(aK_{af}-bK_{ar})}{mv_x^2}-1\right)\hat{\gamma}\\&-\frac{2K_{af}}{mv_x}\delta_f-h_{11}(\hat{\gamma}-\gamma)-h_{12}(\hat{a}_y-a_y)\end{aligned} \tag{18}$$

where h_{11} , h_{12} are the gains of estimation. A particular h_{12} can be chosen to keep the observer robust and estimate the sideslip angle exactly [14].

Thus, the sideslip angle can be fed back to the AFS control. The feedback gain K_γ, K_β in Equation (16) can be determined by linear quadratic regulator (LQR).

4.2 LQR control

LQR can be used to find a control vector $\boldsymbol{u}$ to minimize the cost function J for its good stability and robustness properties [6]. The cost function J of the AFS control takes the form:

$$J = \int_0^t (\boldsymbol{e}^{\mathrm{T}}\boldsymbol{Q}_0\boldsymbol{e} + \boldsymbol{u}^{\mathrm{T}}\boldsymbol{R}_0\boldsymbol{u})dt \tag{19}$$

where $\boldsymbol{e} = \begin{bmatrix} e_1 \\ e_2 \end{bmatrix} = \begin{bmatrix} \beta - \beta_d \\ \gamma - \gamma_d \end{bmatrix}$, $\boldsymbol{u}$ is the control input, $\boldsymbol{Q}_0$ and $\boldsymbol{R}_0$ are the weighting matrices of $\boldsymbol{e}$ and $\boldsymbol{u}$. Minimizing the cost function J , an optimized feedback control input can be obtained:

$$\boldsymbol{u}^* = -\boldsymbol{K}_{lqr}\boldsymbol{x}(\mathrm{t}) = -\boldsymbol{R}_0^{-1}\boldsymbol{B}^{\mathrm{T}}\boldsymbol{P}_0\boldsymbol{x}(\mathrm{t}) \tag{20}$$

where $\boldsymbol{P}_0$ is the result of the Riccati equation $\boldsymbol{P}_0\boldsymbol{A} + \boldsymbol{A}^{\mathrm{T}}\boldsymbol{P}_0 - \boldsymbol{P}_0\boldsymbol{B}\boldsymbol{R}_0^{-1}\boldsymbol{B}^{\mathrm{T}}\boldsymbol{P}_0 + \boldsymbol{Q}_0 = 0$.

LQR provides the optimized feedback gain with the function of system matrices $\boldsymbol{A}$ and $\boldsymbol{B}$. And the system uncertainties have not been dealt with in the linear time-invariant nominal model. However, many factors, such as inflation pressure, normal load, nonlinearity, affect vehicle parameters [14]. As a result, the system will not perform optimally. Although some inherent robustness properties exist; the classical LQR controller is not robust enough to system uncertainties and cannot guarantee the stability of the actual system [15].Therefore, the controller should be modified with regard to parameter uncertainties of the vehicle.

The tire parameters represent the most important source of uncertainties in the vehicles models [16]. The tire cornering stiffness uncertainties can be represented by a linear function with a bounded uncertainty [13].

$$\begin{cases} K_{\alpha f}^* = K_{\alpha f}(1+\sigma_f\delta_1) & \|\delta_1\| \le 1 \\ K_{\alpha r}^* = K_{\alpha r}(1+\sigma_r\delta_2) & \|\delta_2\| \le 1 \end{cases} \tag{21}$$

where σ_f , σ_r are the positive scaling factors reflecting the magnitude of the deviation from the normal values $K_{\alpha f}$ and $K_{\alpha r}$.

Consider a general state equation including external disturbance:

$$\dot{\boldsymbol{x}} = \boldsymbol{A}\boldsymbol{x} + \boldsymbol{B}_1\boldsymbol{u} + \boldsymbol{B}_2\boldsymbol{w} \tag{22}$$

where $\boldsymbol{u}$ and $\boldsymbol{w}$ are the control input and external lateral disturb forces, respectively. Then the uncertain linear system can be described in the following way with the parameter variations:

$$\dot{\boldsymbol{x}}(\mathrm{t}) = [\boldsymbol{A} + \boldsymbol{\Delta A}(\mathrm{t})]\boldsymbol{x}(\mathrm{t}) + [\boldsymbol{B}_1 + \boldsymbol{\Delta B}_1(\mathrm{t})]\boldsymbol{u(t)} + \boldsymbol{B}_2\boldsymbol{w}(\mathrm{t}) \tag{23}$$

where $\boldsymbol{A}$, $\boldsymbol{B}_1$, $\boldsymbol{B}_2$ are normal matrices that describe the system, $\boldsymbol{\Delta A}(\mathrm{t})$, $\boldsymbol{\Delta B}_1(\mathrm{t})$ are perturbed matrices representing time-varying parameter uncertainties.

$$\boldsymbol{A} = \begin{bmatrix} \dfrac{2(K_{af}+K_{ar})}{mv_x} & \dfrac{2(aK_{af}-bK_{ar})}{mv_x^{\,2}} - 1 \\ \dfrac{2(aK_{af}-bK_{ar})}{I_z} & \dfrac{2(a^2K_{af}+b^2K_{ar})}{I_z v_x} \end{bmatrix},$$

$$\boldsymbol{\Delta A} = \begin{bmatrix} \dfrac{2(K_{af}\sigma_f\delta_1+K_{ar}\sigma_r\delta_2)}{mv_x} & \dfrac{2(aK_{af}\sigma_f\delta_1-bK_{ar}\sigma_r\delta_2)}{mv_x^{\,2}} \\ \dfrac{2(aK_{af}\sigma_f\delta_1-bK_{ar}\sigma_r\delta_2)}{I_z} & \dfrac{2(a^2K_{af}\sigma_f\delta_1+b^2K_{ar}\sigma_r\delta_2)}{I_z v_x} \end{bmatrix}$$

$$\boldsymbol{B}_1 = \begin{bmatrix} -\dfrac{2K_{af}}{mv_x} \\ -\dfrac{2aK_{af}}{I_z} \end{bmatrix}, \quad \boldsymbol{B}_2 = \begin{bmatrix} \dfrac{1}{mv_x} \\ \dfrac{l_w}{I_z} \end{bmatrix},$$

$$\boldsymbol{\Delta B}_1 = \begin{bmatrix} -\dfrac{2K_{af}\sigma_f\delta_1}{mv_x} \\ -\dfrac{2aK_{af}\sigma_f\delta_1}{I_z} \end{bmatrix} = \sigma_f\delta_1 \begin{bmatrix} -\dfrac{2K_{af}}{mv_x} \\ -\dfrac{2aK_{af}}{I_z} \end{bmatrix}$$

Taking account of the uncertainties into the LQR control design of the normal system, the Riccati equation and cost function will be extended. The Riccati equation takes the following form:

$$\begin{aligned} &\boldsymbol{P}\boldsymbol{A} + \boldsymbol{A}^{\mathrm{T}}\boldsymbol{P} + \boldsymbol{P}\boldsymbol{\Delta}\mathrm{A} + \boldsymbol{\Delta}\boldsymbol{A}^{\mathrm{T}}\boldsymbol{P} + \frac{\boldsymbol{1}}{\boldsymbol{\varphi}^{\boldsymbol{2}}}\boldsymbol{P}\boldsymbol{B}_2\boldsymbol{B}_2^{\mathrm{T}}\boldsymbol{P} \\ &-(1+\sigma_f\delta_1)^2\boldsymbol{P}\boldsymbol{B}_1\boldsymbol{R}_0^{-1}\boldsymbol{B}_1^{\mathrm{T}}\boldsymbol{P} + \boldsymbol{Q}_0 = 0 \end{aligned} \tag{24}$$

To keep the system robust, $\boldsymbol{P}$ should be constrained as:

$$\begin{aligned} &-\boldsymbol{P}\boldsymbol{A} - \boldsymbol{A}^{\mathrm{T}}\boldsymbol{P} - \boldsymbol{P}\Delta\boldsymbol{A} - \Delta\boldsymbol{A}^{\mathrm{T}}\boldsymbol{P} - \frac{\boldsymbol{1}}{\boldsymbol{\varphi}^{\boldsymbol{2}}}\boldsymbol{P}\boldsymbol{B}_2\boldsymbol{B}_2^{\mathrm{T}}\boldsymbol{P} \\ &+(1+\sigma_f\delta_1)^2\boldsymbol{P}\boldsymbol{B}\boldsymbol{R}_0^{-1}\boldsymbol{B}^{\mathrm{T}}\boldsymbol{P} \ge 0 \end{aligned} \tag{25}$$

Decompose $\boldsymbol{\Delta A}(\mathrm{t})$, $\boldsymbol{\Delta B}_1(\mathrm{t})$ and define the matrices with $\boldsymbol{L}$, $\boldsymbol{N}$ as follows:

$$\boldsymbol{\Delta A} = \boldsymbol{L}\boldsymbol{N}^{\mathrm{T}} \tag{26}$$

Then the sufficient condition for (25) can be expressed as:

$$\begin{aligned} &\boldsymbol{P}\boldsymbol{A} + \boldsymbol{A}^{\mathrm{T}}\boldsymbol{P} + (\boldsymbol{Q}_0 + \lambda\boldsymbol{N}\boldsymbol{N}^{\mathrm{T}}) - \boldsymbol{P}((1+\sigma_f\delta_1)^2\boldsymbol{B}_1\boldsymbol{R}_0^{-1}\boldsymbol{B}_1^{\mathrm{T}} \\ &-\frac{1}{\varphi^2}\boldsymbol{B}_2\boldsymbol{B}_2^{\mathrm{T}} - \frac{1}{\lambda}\boldsymbol{L}\boldsymbol{L}^{\mathrm{T}})\boldsymbol{P} = 0 \end{aligned} \tag{27}$$

where $\boldsymbol{Q}_0, \boldsymbol{R}_0$ are the same as the normal system without uncertainties. The terms with φ are responsible for the external disturbance rejection. The internal disturbance attenuation is taken into account by the terms with λ. Then a positive definite solution $\boldsymbol{P}$ should be found to design the control to guarantee stability and robustness. When a solution $\boldsymbol{P} = \boldsymbol{P}^{\mathrm{T}} > 0$ is found in the Robust Riccati Equation (27), the state weighting matrix $\boldsymbol{Q}_0$ can be modified as:

$$\begin{aligned}\boldsymbol{Q} &= -\boldsymbol{P}\boldsymbol{A} - \boldsymbol{A}^{\mathrm{T}}\boldsymbol{P} + \boldsymbol{P}((1+\sigma_f\delta_1)^2\boldsymbol{B}_1\boldsymbol{R}_0^{-1}\boldsymbol{B}_1^{\mathrm{T}} - \frac{1}{\varphi^2}\boldsymbol{B}_2\boldsymbol{B}_2^{\mathrm{T}})\boldsymbol{P} \\ &= \boldsymbol{Q}_0 + \lambda\boldsymbol{N}\boldsymbol{N}^{\mathrm{T}} + \frac{1}{\lambda}\boldsymbol{P}\boldsymbol{L}\boldsymbol{L}^{\mathrm{T}}\boldsymbol{P}\end{aligned} \tag{28}$$

With the state weighting matrix $\boldsymbol{Q}$, the cost function can be modified and the control gain can be obtained.

5 HILS system design

To evaluate the designed controller, some real-time simulations are performed with the designed steering equipment for the AFS system. The hardware-in-the-loop simulation (HILS) integrates the actual ECU and its peripheral hardware with the virtual vehicle model, forming a closed loop to be simulated in real time [17].

5.1 HILS system

Fig.7 shows the experimental equipment which is made from an AFS unit with a reactive module. The HILS system consists of three parts: the hardware which includes steering system mechanics, ECU, motor, data acquisition card, sensors, PCs; the software part which includes the nonlinear vehicle model in MATLAB, the AFS control logics, and post-processing module; and interface part which links the hardware and software parts.

Fig.7. Hardware-in-the-loop-Simulation system

In the HILS system, both the steering angles of the driver and the assist motor are applied to move the steering linkages, whose displacement is measured by the sensor. With the sensor signal, the vehicle model resides in the PC is computed, then yaw rate and sideslip angle signals are sent back to the ECU as the feedback. Thus, the desired assist angle can be obtained to control the motor.

5.2 Nonlinear vehicle model

In the HILS system, a two-track nonlinear vehicle model, which has been validated against test data in our previous study, is presented to simulate and evaluate the proposed AFS controller. The model is derived through neglecting heave, roll and pitch motions, as in Fig.8 [18]. The longitudinal direction is ignored because only the lateral stability is of interest in this study. However, the extra moment produced by the unbalanced longitudinal forces is covered in the model according with the crosswind.

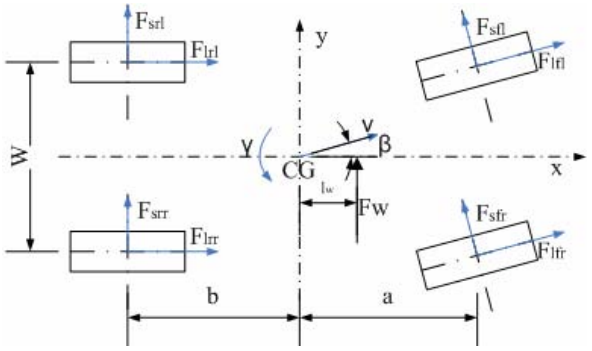

Fig.8. Vehicle model and external forces

The equations of lateral and yaw motions for the vehicle model are derived:

$$\begin{aligned}m(\dot{v}_y + v_x\gamma) = &(F_{yfl} + F_{yfr})\cos\delta_f + F_{yrl} + F_{yrr} \\ &+ (F_{xfl} + F_{xfr})\sin\delta_f + F_w\end{aligned} \tag{29}$$

$$\begin{aligned}I_z\dot{\gamma} = &((F_{yfl} + F_{yfr})\cos\delta_f + (F_{xfl} + F_{xfr})\sin\delta_f)a + l_wF_w \\ &-(F_{yrl} + F_{yrr})b + ((F_{xfr} - F_{xfl})\cos\delta_f + F_{xrr} - F_{xrl})\frac{W}{2}\end{aligned} \tag{30}$$

where $F_{lfl}, F_{lfr}, F_{lrl}, F_{lrr}$ (F_{li}) are the longitudinal forces on the front left, front right, rear left, rear right tyres, respectively; $F_{sfl}, F_{sfr}, F_{srl}, F_{srr}$ (F_{si}) the lateral forces on the front left, front right, rear left, rear right tyres; v_y the lateral velocity; W the track width, F_w the crosswind force, l_w the distance from the gravity centre to the action point of crosswind force.

The cornering stiffness uncertainty is considered using the nonlinear tyre model. As in the vehicle model, the tyre force of each wheel can be computed by the tyre model. In order to simulate the performance of the tyres, the nonlinear Dugoff model is employed [19]. The simplified model is denoted as [20, 21]:

$$F_{yi} = \frac{K_{\alpha i} \tan \alpha_i}{1 - s_i} f(\eta), \quad F_{xi} = \frac{K_{xi} s_i}{1 - s_i} f(\eta) \quad (31)$$

with $\eta = \frac{\mu F_{zi}(1 - s_i)[1 - \varepsilon_r v_{xi} \sqrt{s_i^2 + \tan^2 \alpha_i}]}{2\sqrt{K_{xi}^2 s_i^2 + K_{\alpha i}^2 \tan^2 \alpha_i}}$, i denotes the different tyre, $f(\eta) = \begin{cases} \eta(2 - \eta) & \eta < 1 \\ 1 & \eta > 1 \end{cases}$.

where K_α is the cornering stiffness of each tyre, also expressed as K_1, K_2 for front, rear tyres respectively; K_s the longitudinal stiffness of each tyre, ε_r the road adhesion reduction factor, F_{zi} the vertical load acting on each wheel, s the slip ratio, α the slip angle of each wheel.

According to the nonlinear vehicle model, each wheel has an independent slip angle:

$$\alpha_{fl} = \delta_f - \arctan\left(\frac{v_y + a\gamma}{v_x - W\gamma/2}\right) \quad (32a)$$

$$\alpha_{fr} = \delta_f - \arctan\left(\frac{v_y + a\gamma}{v_x + W\gamma/2}\right) \quad (32b)$$

$$\alpha_{rl} = \arctan\left(\frac{b\gamma - v_y}{v_x - W\gamma/2}\right) \quad (32c)$$

$$\alpha_{rr} = \arctan\left(\frac{b\gamma - v_y}{v_x + W\gamma/2}\right) \quad (32d)$$

The instantaneous vertical load F_{zi} is the sum of the static tyre load and load transfer. In addition, the load transfer is caused by longitudinal and lateral acceleration. Then the vertical load for each wheel can be expressed as [22]:

$$F_{zfl} = \frac{1}{2(a+b)}\left(mgb - m\dot{v}_x h + \frac{2mv_x(\dot{\beta} + \gamma)h}{W} b\right) \quad (33a)$$

$$F_{zfr} = \frac{1}{2(a+b)}\left(mgb - m\dot{v}_x h - \frac{2mv_x(\dot{\beta} + \gamma)h}{W} b\right) \quad (33b)$$

$$F_{zrl} = \frac{1}{2(a+b)}\left(mga + m\dot{v}_x h + \frac{2mv_x(\dot{\beta} + \gamma)h}{W} a\right) \quad (33c)$$

$$F_{zrr} = \frac{1}{2(a+b)}\left(mga + m\dot{v}_x h - \frac{2mv_x(\dot{\beta} + \gamma)h}{W} a\right) \quad (33d)$$

As the friction coefficient μ is an important parameter of cornering stiffness and necessary in the AFS control, it is assumed that this parameter is known, or can be estimated by other means [21, 23].

6 Simulation results

The performance of the designed AFS controller is tested in the HILS system and compared with the conventional vehicle without AFS control. The lateral acceleration, which has been utilized to the sideslip estimation, is used in the result comparison instead of sideslip angle.

6.1 Torque assistant maneuver

In Fig.9, a sine wave steering is inputted at the speed of 60 km/h where the required VSR is the same as the ratio of mechanical system. (a) plots the steering torque versus steering wheel angle of the AFS controlled vehicle and the conventional vehicle without AFS. (b), (c) are the lateral acceleration and yaw rate responses, respectively.

It can be seen that, in order to track the similar yaw rate and lateral acceleration, the steering torque provided by the driver is reduced by the torque compensation in active steering operation. Therefore, the effectiveness of torque compensation by EPS actuator is confirmed.

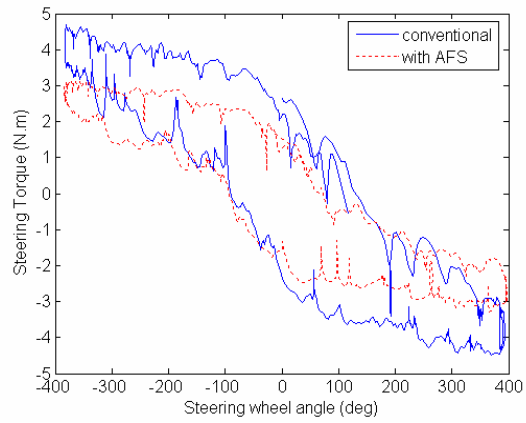

(a) Steering torque vs. steering wheel angle

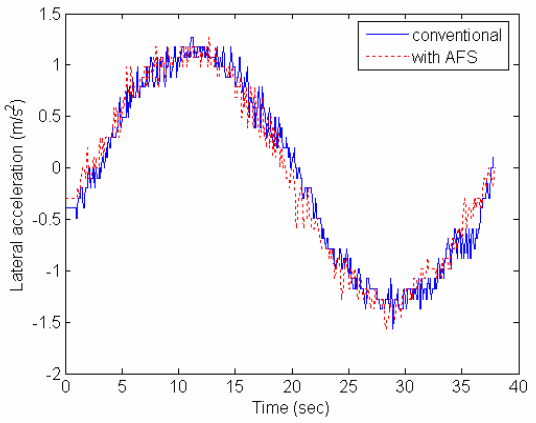

(b) Lateral acceleration

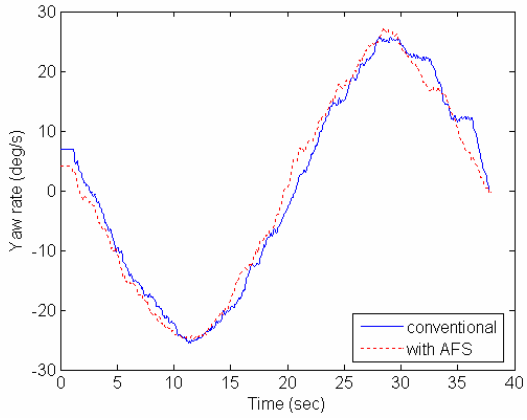

(c) Yaw rate

Fig.9. Responses of the torque assistant maneuver.

6.2 Lane keeping steering maneuver

The sine wave steering maneuver was tested on the wet road with μ = 0.5 at the speed of 25 km/h, as shown in Fig.10. To demonstrate the AFS effectiveness, similar steering wheel inputs as shown in (a) are provided to the AFS controlled vehicle and conventional vehicle without AFS, respectively.

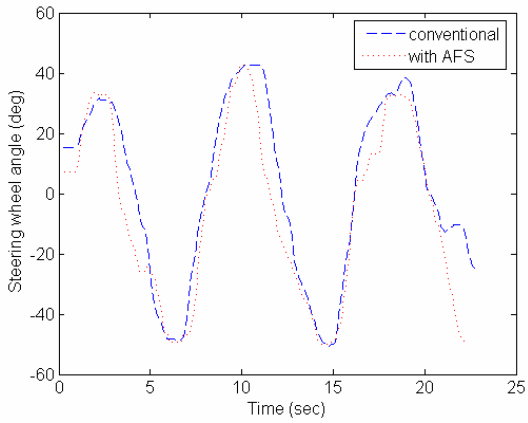

(a) Steering wheel angle

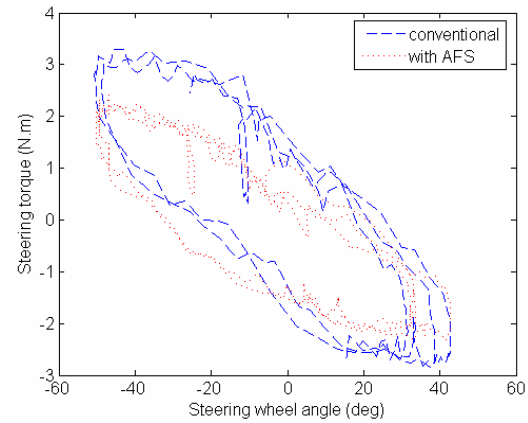

(b) Steering torque vs. steering wheel angle

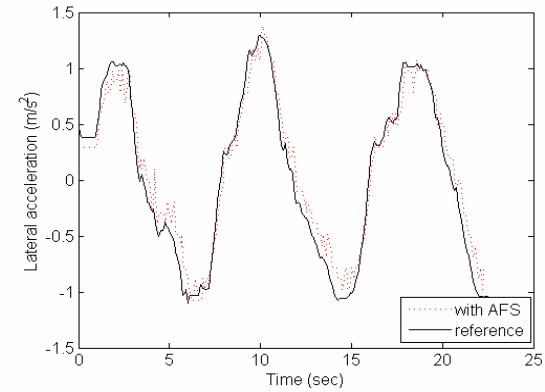

(c) Lateral acceleration (AFS vehicle vs. reference)

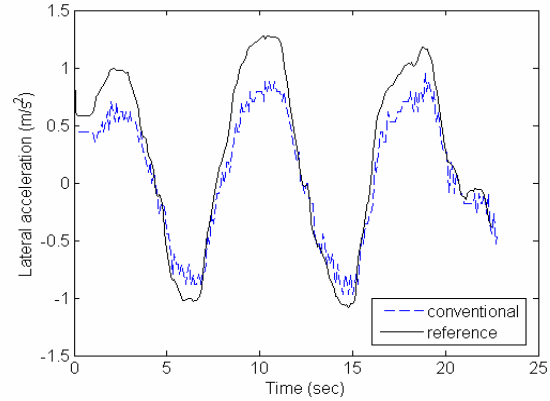

(d) Lateral acceleration (conventional vs. reference)

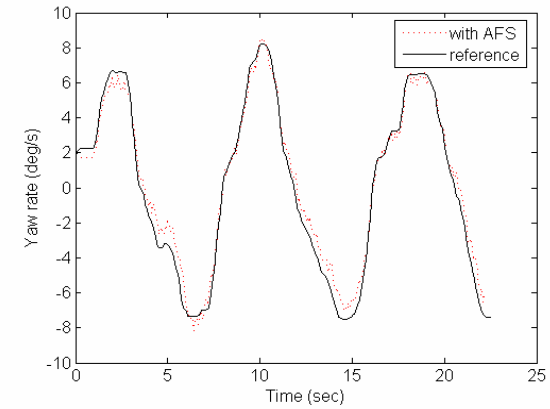

(e) Yaw rate (AFS vehicle vs. reference)

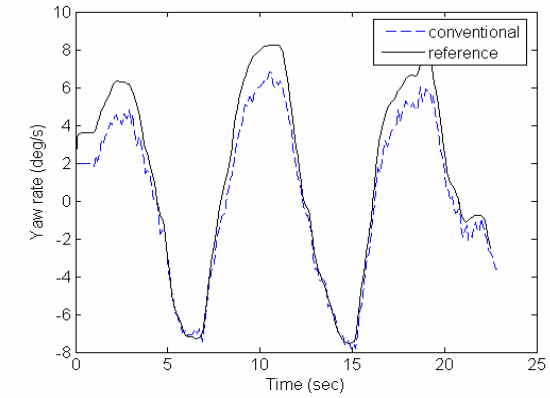

(f) Yaw rate of conventional vehicle vs. reference

Fig.10. Responses of the lane keeping maneuver.

The AFS controlled vehicle is seen to require smaller torque with the comparison in (b). Figure (c) and (e) are the lateral acceleration and yaw rate responses of the AFS controlled vehicle; (d) and (f) are the lateral acceleration and yaw rate responses of the conventional vehicle. The reference signals to the corresponding inputs determined by Equation (14) and (15) are also included in them.

Results indicate that both the lateral acceleration and the yaw rate of the AFS controlled vehicle follow the reference signals in a reasonably closer fashion than conventional vehicles. The maximum lateral acceleration deviation from the reference response is 0.18 m/s^2 for the AFS controlled vehicle, while 0.56 m/s^2 for the conventional vehicle. The maximum yaw rate deviation from the reference response is 1.04 deg/s for the AFS controlled vehicle, while 2.5 deg/s for the conventional vehicle.

6.3 Braking on a split road surface

During braking, additional yaw moment will be produced when asymmetric forces are applied to left and right side wheels. Then the additional yaw moment will result in vehicle instability. A particular condition of asymmetric braking is emergency braking on split adhesion road. To stop the vehicle as quickly as possible in emergency, the maximal braking forces without locking the wheels are applied to the wheels. With different adhesion conditions on the left and right sides, a yaw moment will be generated and push the vehicle to the side where the friction coefficient is higher. In case of braking on a split surface, compatibility between stability and braking performance is impossible using only longitudinal force [18]. The AFS can correct the instability with angle compensation automatically according to the feedback of yaw rate and sideslip angle.

To illustrate the effectiveness of this developed AFS system, the driver strives to provide no stability compensation to the front steering wheels. The test was conducted with the initial velocity of 60 km/h. Fig.11 shows the result of straight braking on split road with the road adhesion coefficient of left side is 0.5, and right side 0.7. The lateral acceleration and yaw rate are shown in (a) and (b).The peak yaw rate and lateral acceleration of the AFS controlled vehicle are smaller than the conventional vehicle. Thus, conclusion can be drawn that the stability is improved with the AFS control.

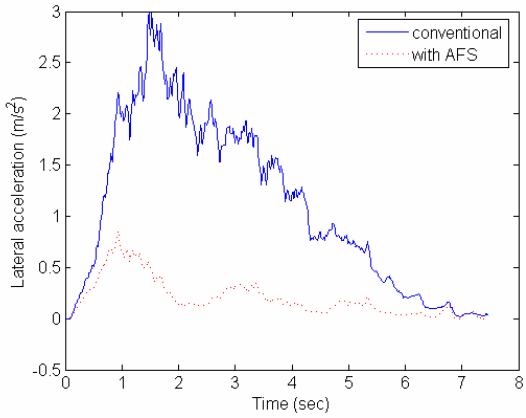

(a) Lateral acceleration

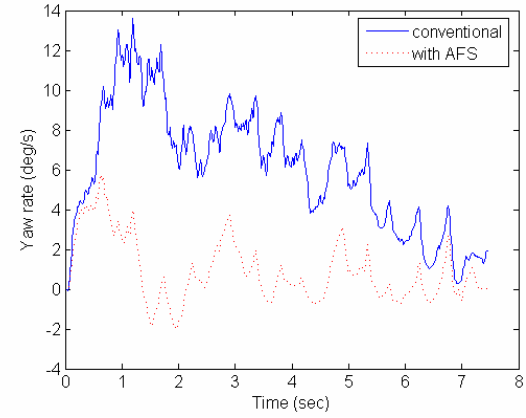

(b) Yaw rate

Fig.11. Responses of split braking maneuver.

7 Conclusions

In this paper, a new developed active front steering (AFS) system control has been presented. On the basic of the C-EPS mechanism, the proposed AFS system can control the EPS actuator to compensate the occurred reaction steering torque simultaneously when the AFS actuator operates. Starting with the construction presentation, a mathematical model for the AFS system was derived. Afterwards, the task of the AFS controller design proceeded in two parts: one is the EPS actuator control to reduce the steering torque requirement to the driver, the other is to provide the compensated steering angle for steering affect and vehicle stability. In contrast to the conventional stability control, both the sideslip angle and the yaw rate have been fed back to improve the vehicle stability. In addition, the tire stiffness uncertainties have been dealt with to provide the control robustness. To demonstrate the performance of the designed AFS controller, HILS tests were conducted in three test maneuvers with both the AFS controlled vehicle and the conventional vehicle without AFS. Test results

show that the proposed controller can effectively alleviate the reaction steering torque as well as reduce the deviation from the desired response. The AFS system can improve the vehicle stability and maneuverability evidently.

Reference:

[1] Klier, W., Reimann, G. and Reinelt, W., Concept and functionality of the active front steering system, *SAE Technical paper*, 2004, No.2004-21-0073.

[2] Koehn, P. and Eckrich, M., Active steering - the BMW approach towards modern steering technology, *SAE Technical paper*, 2004, No.2004-01-1105.

[3] Hosaka, M. and Murakami, T., Yaw rate control of electric vehicle using steer-by-wire system, *IEEE Technical paper*,2004, pp.31-34.

[4] Yih, P., Steer-by-wire implications for vehicle handling and safety, PhD dissertation, Stanford University, 2005.

[5] Douglas, J. and Athans, M., Robust linear quadratic designs with real parameter uncertainty. *IEEE Transactions on automatic control*, Vol.39, No.1, 1994, pp.107-111.

[6] Gianone, L., Palkovics, L. and Bokor, J., Design of an active 4WS system with physical uncertainties, *Control Eng. Practice*, Vol.3, No.8, 1995, pp.1075-1083.

[7] Kim, J.H. and Song, J.B., Control logic for an electric power steering system using assist motor, *Mechatronics* Vol.12, 2002, pp.447–459.

[8] Khan,W. and Taylor,D., Adaptive control of ac motor drives with inverter nonlinearities, *International Journal of Control*, Vol.72, No.9, 1999, pp.784-798.

[9] Chen, D.L., Yin, C.L. and Chen, L., Study on active front steering based on state-space observer, *China Mechanical Engineering* Vol.18, No.24, 2007, pp. 3019-3023.

[10] Song, J.H., Boo, K.S., Kim, H.S. et al., Model development and control methodology of a new electric power steering system, *Proc. Instn Mech. Engrs Part D: J. Automobile Engineering*, Vol. 218, 2004, pp.967–975.

[11] Liu, Z., Research on dynamic analysis and control method of electric power assisted steering system for vehicle, PhD dissertation, Huazhong University of Science and Technology, 2004.

[12] Mammar, S. and Baghdassaria, V.B., Two-degree-of-freedom formulation of vehicle handling improvement by active steering, *Proceedings of the American Control Conference*, 2000.

[13] Mammar, S. and Koenig, D., Vehicle handling improvement by active steering, *Vehicle System Dynamics*, Vol. 38, No.3, 2002, pp.211-242.

[14] Aoki, Y. and Hori, Y., Robust design of body slip angle observer for electric vehicles and its experimental demonstration, *Electrical Engineering in Japan*, Vol. 159, No. 1, 2007 (Translated from Denki Gakkai Ronbunshi, Vol. 125-D, No. 5467–472, 2005).

[15] Li, P., Chen, N. and Sun, Q.H., Optimal follow up control of 4WS vehicle based on state estimator, *Chinese Journal of Mechanical Engineering*, Vol.40 No.1, 2004, pp.50-55.

[16] Azad, N.L., Khajepour, A.and Mcphee, J., Robust state feedback stabilization of articulated steer vehicles, *Vehicle System Dynamics*, Vol. 45, No. 3, 2007, pp.249–275.

[17] Park, K. and Heo, S.J., Development of hardware-in-the-loop simulation system for use in design and validation of VDC logics, *International Journal of the Korean Society of Precision Engineering*, Vol. 4, No. 3, 2003, pp.28-35

[18] Guvenc,B.A, Acarman, T. and Guvenc, L., Coordination of steering and individual wheel braking actuated vehicle yaw stability control, *IEEE Technical paper*, 2004, pp.288-293

[19] Hiraoka, T., Kumamoto, H. and Nishihara, O., Sideslip angle estimation and active front steering system based on lateral acceleration data at centers of percussion with respect to front/rear wheels. *JSAE Review* Vol.25, 2004, pp.7-42

[20] Dugoff, H., Fancher, C., Segel, L., An analysis of tire traction properties and their influence on vehicle dynamics performance, *SAE Technical paper*, No. 700377, 1970, pp.1219-1243.

[21] Kwak, B., Park, Y.J. and Kim, D.S., Design of observer for vehicle stability control system, *FISITA World Automotive Congress*, 2000.

[22] Alejandro, D. Dominguez-Garcia, John G. Kassakian, Joel E. Schindall., A backup system for automotive steer-by-wire, actuated by selective braking, *35th IEEE Power Electronics Specialists Conference*, 2004, pp.383-388.